The effect of non-contact electro capacitive cancer therapy on DMBA-induced rat breast tumor angiogenesis

Endah Sri Palupi[1,2], Bambang Retnoaji[3], Pudji Astuti[4], Firman Alamsyah[5,6], Warsito Purwo Taruno[6], Rarastoeti Pratiwi[7,*]

[1]Postgraduate Program, Faculty of Biology, Universitas Gadjah Mada
[2]Animal Structure and Development Laboratory, Faculty of Biology, Universitas Jenderal Soedirman, Purwokerto, Indonesia
[3]Animal Structure and Development Laboratory, Faculty of Biology, Universitas Gadjah Mada
[4]Department of Physiology, Faculty of Veterinary, Universitas Gadjah Mada
[5]Faculty of Science and Technology, Universitas Al Azhar Indonesia, Jakarta, Indonesia
[6]Center for Medical Physics and Cancer Research, Ctech Labs Edwar Technology, Tangerang
[7]Biochemistry Laboratory, Faculty of Biology, Universitas Gadjah Mada
*Corresponding author: rarastp@ugm.ac.id

ABSTRACT Alternating Current-Electric Field (AC-EF) generated by non-contact Electro Capacitive Cancer Therapy (ECCT) can inhibit breast tumor growth. However, its effect on breast tumor angiogenesis remains unclear. Since angiogenesis is involved in normal physiology and tumors, it is crucial to investigate the effect of ECCT on normal and breast tumor angiogenesis. Samples consisting of rat breast normal tissue and breast tumors were obtained from the biobank, with tumors induced by 7,12-dimethylbenz (α) anthracene (DMBA) at 20 mg/kg BW 10 times over five weeks. Meanwhile, ECCT exposure of 150 kHz and 18 Vpp was conducted for 21 days at 10 hours/day. The qPCR method was used for gene expression analysis, while immunohistochemistry used antibody anti-Vegfr2 that was used to detect Vegfr2 protein expression. Data were analyzed using one-way ANOVA and t-tests performed with GraphPad Prism ver.9.5.1 software. The results revealed no impact of ECCT exposure on normal breast tissue angiogenesis. Interestingly, there was a significant increase in the number of blood vessels following the upregulation of Vascular Endothelial Growth Factor Receptor-2 (*Vegfr2*) as opposed to its primary signal, Vascular Endothelial Growth Factor-A (*Vegfa*). Furthermore, gene expression of Hypoxia Inducible Factor-1α (*Hif1α*) and Specificity Protein-1 (*Sp1*) was similar to that of the control group, suggesting that Vegfr2-dependent angiogenesis regulates ECCT-treated breast tumor angiogenesis.

KEYWORDS AC electric field; Angiogenic gene; Breast cancer; Vegfr2-dependent angiogenesis

1. Introduction

Angiogenesis is the new blood vessels' development from pre-existing ones to facilitate nutrient and gas transport, and the advanced tumor needs angiogenesis for metastasis (Zimna and Kurpisz 2015). This mechanism is involved in normal physiology and pathological conditions, e.g., breast tumors. In breast tumors and other tumor types, angiogenesis is one of the cancer hallmarks (Hanahan 2022; Hanahan and Weinberg 2000). Thus, blocking angiogenesis may inhibit tumor growth.

As the most dominant tumor in women, breast tumors (Sung et al. 2021) have become a major target of anti-cancer devices, i.e., Electro Capacitive Cancer Therapy (ECCT) (Alamsyah et al. 2015, 2018; Pratiwi et al. 2019; Alamsyah et al. 2021). ECCT is a non-contact anti-cancer device for cancer treatment, employing a low to an intermediate frequency (<300 kHz) and low intensity

(<30 Vpp) (Alamsyah et al. 2015, 2018; Pratiwi et al. 2019; Alamsyah et al. 2021). This device was designed by Dr. Warsito P. Taruno from Indonesia (IDN Patent REG P00201200011, 2012).

The ECCT effectiveness for breast tumor treatment has been investigated *in vitro* and *in vivo* as an anti-mitotic and pro-apoptotic device without reported side effects. These capacities have been proven by ECCT of 150 kHz and 18 Vpp (Pratiwi et al. 2019) and ECCT of 100 kHz and 18 Vpp (Alamsyah et al. 2015, 2018, 2021), but there was no information on those effects on breast tumor angiogenesis. Related to angiogenesis, previous research using Tumor Treating Field (TTField), a similar device with ECCT, has downregulated Vascular Endothelial Growth Factor (*Vegf*), Hypoxia Inducible Factor-1α (*Hif1α*), Matrix Metalloproteinase-2 (MMP2), and Matrix Metalloproteinase-9 (MMP9) in glioblastoma cell culture (Kim et al. 2016). VEGF along with MMP-9 serve impor-

tant roles in the angiogenesis and invasion that contribute to tumor metastasis (Guntarno et al. 2021).

Considering previous studies, ECCT may have an anti-angiogenic capacity. ECCT of 150 kHz and 18 Vpp has downregulated Interleukin-18 (*IL18*) and C-C Motif Chemokine Ligand 2 (*CCL2*) (Pratiwi et al. 2019), which *IL18* may promote angiogenesis (Kobori et al. 2018). This result shows that ECCT may inhibit blood vessel development through different pathways. Thus, further research is necessary. Furthermore, the investigated Alternating Current (AC) electric field device provided evidence as anti-angiogenic only by inhibiting the pro-angiogenic signals, excluding its receptor.

Since the introduction of ECCT, several studies have focused on anti-cancer capacity through anti-mitotic and pro-apoptotic activities. However, considering the complex mechanism of cancer and the involvement of angiogenesis in any physiological process, it becomes crucial to investigate any cancer-related treatment effect on angiogenesis. Therefore, this research aimed to investigate the impact of ECCT on the *Hif1α*, Specificity Protein 1 (*SP1*), *Vegfa*, and Vegf receptor 2 (*Vegfr2*) expression in normal and breast tumor angiogenesis. This result may complete pre-clinical data for further clinical research to support ECCT as a novel breast tumor treatment modality.

2. Materials and Methods

2.1. Animals

This is an experimental research, used breast normal and breast tumor tissue samples from the Biobank, stored in RNAlater solution (Invitrogen; cat. no. AM7024) at -20 °C for molecular assay and stored in Neutral Buffer Formalin (NBF, Bio-Optica; cat. no. 05-K01004) for immunostaining. The procedures of animal model preparation were conducted according to (Pratiwi et al. 2019). It was carried out at the animal house of LPPT Research Center Universitas Gadjah Mada, accredited by ISO/IEC 17025:2000. Experimental treatments have been legalized by Ethical Clearance certificate number 00029/04/LPPT/2018. A total of 24 rats (*Rattus norvegicus* Berkenhout, 1769), Sprague–Dawley strain, five weeks old and weighing 50–80 g, were divided into four groups. A 5-day acclimatization was done before treatment. The experimental group of four treatments (including the control group) is shown in Table 1.

Oral DMBA (Sigma–Aldrich; cat. no. D3254-1G) administration dose was 20 mg/kg body weight, given two times a week for five weeks. Palpation was done every two days after DMBA administration. Tumor nodules were observed between 4 and 6 weeks after DMBA induction, and the diameter was measured every two days using a digital caliper (Fisher Scientific).

ECCT cage (designed by Ctech Labs Edwar Technology, IDN Patent REG. P00201200011) is designed for an individual rat. The rats with solid breast tumors (±1 cm

TABLE 1 Experimental design of each treatment group.

No.	Treatment groups	DMBA	ECCT
1	NINT (control)	-	-
2	NIT	-	√
3	INT	√	-
4	IT	√	√

NINT= non-DMBA-induced, non-ECCT-therapied rats; NIT= non-DMBA-induced with ECCT-therapied rats; INT= DMBA-induced, non-ECCT-therapied rats; IT= DMBA-induced with ECCT-therapied rats.

in diameter) were treated with ECCT of 150 kHz and 18 Vpp. ECCT therapy was performed for 21 days (d), 10 hours (h) per day with 2 h of rest (from 06:00 to 11:00 a.m. and continued at 01:00 to 06:00 p.m.). The rats were fed a standard diet and cucumber during ECCT therapy, while a standard diet and water were used during the rest period. Both feedings were *ad libitum*. After ECCT therapy, euthanasia was done using ketamine hydrochloride (Ketalar, Pfizer; cat. no. 629-24006) injection at doses of 150 mg/kg body weight. Glandula mammary and tumor nodule were collected and preserved in RNAlater solution before total RNA extraction and NBF for histological examination.

2.2. Primer design

Hif1α, Sp1, Vegfa, Vegfr2, and *Gapdh* primers were designed and evaluated using bioinformatics tools. The FASTA sequence was obtained from (https://www.ncbi.nlm.nih.gov/). Primer3Plus free access software (https://www.bioinformatics.nl/cgi-bin/primer3plus/primer3plus.cgi) for primer design. The primer sequences were analyzed prior to the ordering, based on several criteria such as melting temperature (http://frodo.wi.mit.edu/ recommended by Bio-Rad qPCR kit), GC content, and gene specificity (https://www.ncbi.nlm.nih.gov/tools/primer-blast/), primer dimer (http://www.primer-dimer.com/), and primer hairpin (http://biotools.nubic.northwestern.edu/OligoCalc.html).

This study used a qPCR kit, SsoFastTM EvaGreen Supermix (Bio-Rad; cat. no. 172-5201), suggesting primer concentration ranged from 300–500 nMol. Primer sequence optimization was done for annealing temperature and primer concentration. The annealing temperature ranged from 56 to 62 °C with a gradient of 6.0. This optimization used a primer concentration of 500 nM. Afterward, the optimum annealing temperature was used for primer concentration optimization, as recommended by the qPCR kit. Primer concentrations for forward and reverse were 300 nM, 400 nM, and 500 nM. Thus, nine combinations of forward and reverse primers were analyzed. The validation of qPCR results was 2% agarose gel electrophoresis.

2.3. Quantitative-RT-PCR

Quantitative-RT-PCR (qRT-PCR) was performed to measure *Hif1α, Sp1, Vegfa*, and *Vegfr2* mRNA expression us-

TABLE 2 Primer sequence for qPCR method.

Gene	Primers	Annealing Temperature/AT (°C)
GAPDH (NM_017008.4)	F: 5'AGACAGCCGCATCTTCTTGT3' R: 5'TTCCCATTCTCAGCCTTGAC3'	Following AT of target genes
HIF1α (NM_024359.2)	F: 5'TGCTCATCAGTTGCCACTTC3' R: 5'CCATCCAGGGCTTTCAGATA3'	56.4
SP1 (NM_012655.2)	F: 5'CAGTTGCTTTGGGAGAGGAG3' R:5'GCTCAACCTCAAAGCTGGTC3'	63.0
VEGFA (NM_001287107.1)	F: 5'GCCTCAGGACATGGCACTAT3' R:5'GGAGGAGGAGGAGCCATTAC3'	61.0
VEGFR2 (NM_013062.2)	F: 5'CAGAAGAGGGACCTCAGACG3' R:5'AGGATAGAGCCGCTGTTTGA3'	59.8

ing a qPCR kit. This step was initiated by RNA isolation with Direct-zol RNA purification kit (Zymo Research; cat. no. R2071), followed by cDNA synthesis using iScript cDNA Synthesis kit (Bio-Rad; cat. no. 1708891). The cDNA template contained an RNA concentration of 500 ng/µL. Primers were as listed in Table 2.

The following steps were pre-denaturation at 95 °C for 30 seconds (s); denaturation at 95 °C for 5 s; annealing (listed in the Table 2); elongation from 65 °C to 95 °C for 5 s; and increment of 5 °C. CFX96 Touch Real-Time PCR Bio-Rad Detection System (Bio-Rad Laboratories, Hercules, CA, USA) was used for qPCR analysis. The relative gene expression data were analyzed using the Livak method (Livak and Schmittgen 2001).

2.4. Histological examination

All samples were processed using the paraffin method following the procedures in Bancroft (Suvarna et al. 2012). In brief, samples were washed and dehydrated using gradually increased alcohol concentration from 70%–100%. Subsequently, it was cleared with Toluene (Merck; cat. no. 1083252500) overnight. The samples were infiltrated using paraffin (Merck; cat. no. 1073372500) at 65 °C and embedded using fresh paraffin. The paraffin block samples were sectioned using a microtome (Microm HM 315) with 4–6 µm thickness and affixed on a Poly-L-lysine coated slide.

2.5. Immunohistochemistry

Immunostaining was performed on INT and IT groups following the protocol of the kit kit (Starr Trek Universal- HRP Detection Kit, Biocare Medical; cat.no. STUHRP700H-KIT). Firstly, the samples were deparaffinized by immersed in xylene (Merck; cat. no. 1086612500) for 30 min and rehydrated using downgraded alcohol concentration (100%–50%). Afterward, samples were heated in citrate buffer pH 6.0 for 15 min at 95 °C in microwaves for antigen retrieval, continued by soaking the slides in the solution of 3% and 0.3% H_2O_2 (Sigma-Aldrich) in methanol, to block endogenous peroxidase, while Background Sniper for 45 min to block non-specific binding. Subsequently, samples were incubated with anti-Vegfr2 (Abcam; cat.no. ab39638) at 4 °C overnight. The antibody was diluted with BSA-PBST 1:100. The following process was continued by Trekkie Universal Link (a universal, affinity-purified, biotinylated secondary antibody) for 60 min of incubation. Then, Trek Avidin HRP Label and DAB Betazoid Chromogen were for 60 and 30 min, respectively, for staining development, followed by counterstaining with Hematoxylin (made from Hematoxylin Krist C.I.75290, Merck; cat. no.1159380025, using Erlich's formulation). Lastly, samples were dehydrated with up-graded alcohol concentration, cleared with xylene, and mounted with Entellan (Merck; cat. no. 1079600500) and coverslip. Control for IHC kit was performed using anti-β tubulin. IHC slides were observed under the Leica ICC50 E microscope with 30 fields of view per replication.

2.6. Statistical analysis

The IHC data were counted and analyzed using ImageJ software, the image processing program developed by the National Institutes of Health. The *Hif1α, Sp1,* and *Vegfa* expression were analyzed statistically using ANOVA (α = 0.05) and continued with the Tukey test. An independent t-test was used for *Vegfr2* expression and the number of blood vessels. Both tests were performed using GraphPad Prism 9.5.1 software, the data analysis and visualization software for scientific research.

3. Results and Discussion

3.1. The effect of ECCT on the Hif1α, Sp1, and Vegfa expressions in the rat breast tissue and breast tumor

Relative gene expression of *Hif1α, Sp1,* and *Vegfa* was shown in Figure 1. The results showed that ECCT exposure has no impact ($p>0.05$) on *Hif1α, Sp1,* and *Vegfa* gene expression of normal breast tissue (NIT group). The *Vegfa* gene expression was noted to increase significantly ($p<0.05$) in the INT group (3.36-fold change) compared to the NINT group. It was consistent with *Hif1α* gene expression in the INT group (6.82-fold change) as compared to the NINT group (P<0.01). The *Vegfa* gene expression was found to be significantly lower ($p<0.05$) in the IT group (1.62-fold change) compared to the INT group (3.36-fold change). However, the decrease of *Hif1α* in the IT group (6.32-fold change) was insignificant compared to the INT
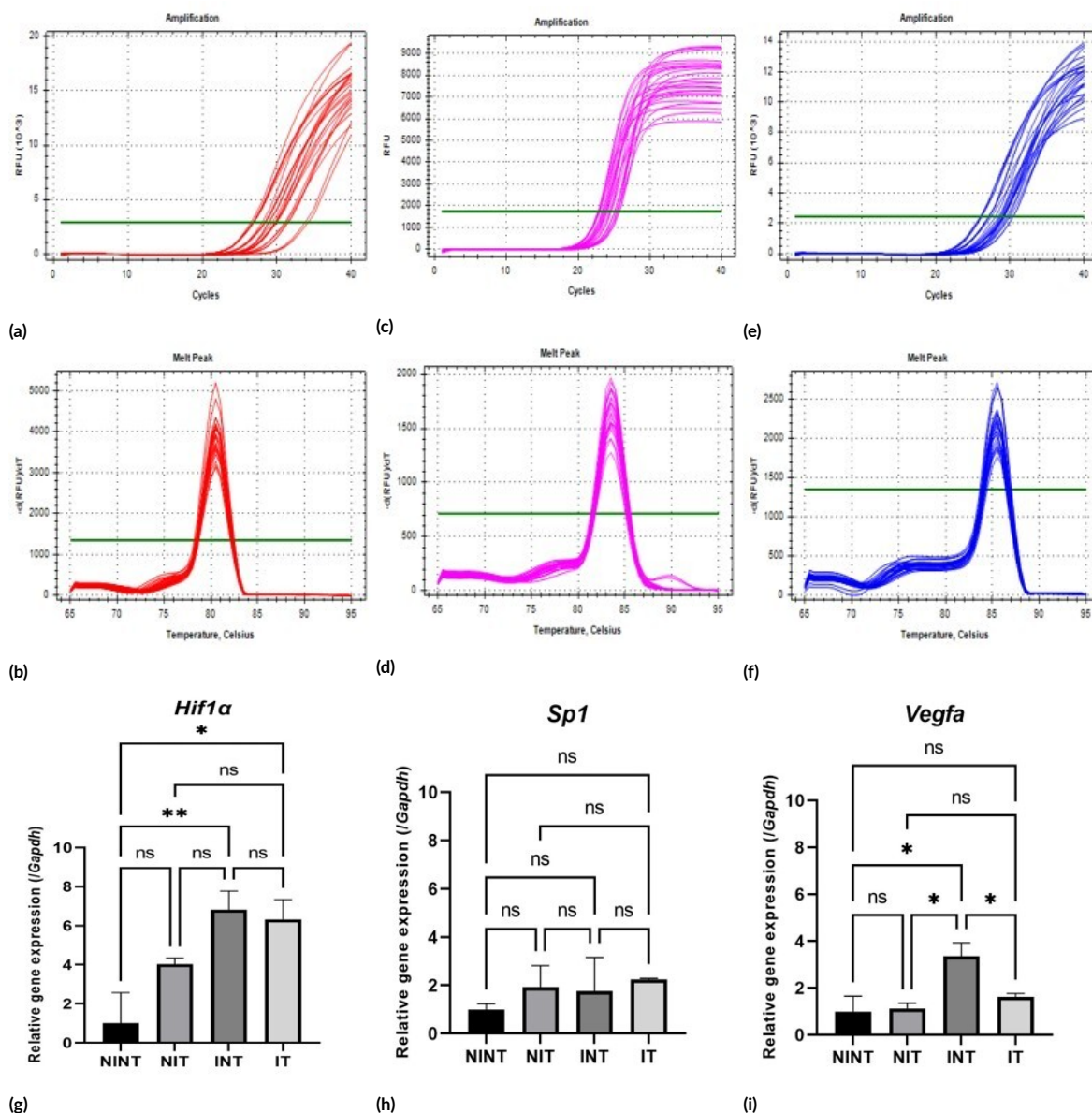
FIGURE 1 Relative gene expression of *Hif1α*, *Sp1*, and *Vegfa* in breast tumor after ECCT therapy. Amplification and melt peak chart of *Hif1α* (1a and 1b), *Sp1* (1c and 1d), and *Vegfa* (1e and 1f). Relative gene expression of *Hif1α* (1g), *Sp1* (1h), and *Vegfa* (1i). The internal control of relative gene expression is Gapdh. ANOVA, α=0.05; ns = not significant; *$p<0.05$; **, $p<0.01$. NINT= non-DMBA-induced, non-ECCT-therapied rats; NIT= non-DMBA-induced, ECCT-therapied rats; INT= DMBA-induced, non-ECCT-therapied rats; IT= DMBA-induced and ECCT-therapied rats. The error bar indicates a standard deviation of three biological replications with two technical replications.

group (6.82-fold change). Furthermore, the groups have no significant difference in *Sp1* gene expression. It suggests that only the *Vegfa* mRNA expression in breast tumors was downregulated significantly by ECCT exposure in comparison without ECCT therapy.

3.2. The effect of ECCT on the Vegfr2 expression in the rat breast tissue and breast tumor

The relative gene expression of *Vegfr2* was shown in Figure 2. The *Vegfr2* gene expression in normal rat breast tissue with ECCT exposure (NIT) was similar to those without ECCT (NINT). Besides that, *Vegfr2* expression was barely increased in the ECCT-treated breast tumors (IT group) (2.15-fold change) compared to the untreated

(INT group) (P>0.05). The in-line result was also indicated in Vegfr2 protein expression, which was upregulated after ECCT exposure (P<0.05) (Figure 3).

3.3. The effect of ECCT on the Vegfr2 expression in the rat breast tumor

The appearance of Vegfr2 protein expression in breast tumors, both with (IT) and without ECCT exposure (INT), was shown in Figure 3a. The number of Vegfr2-positive cells in the IT group was significantly higher than INT ($p<0.0001$) (Figure 3b), as well as the number of blood vessels (Figure 3b). These increasing results were consistent with the *Vegfr2* gene expression.
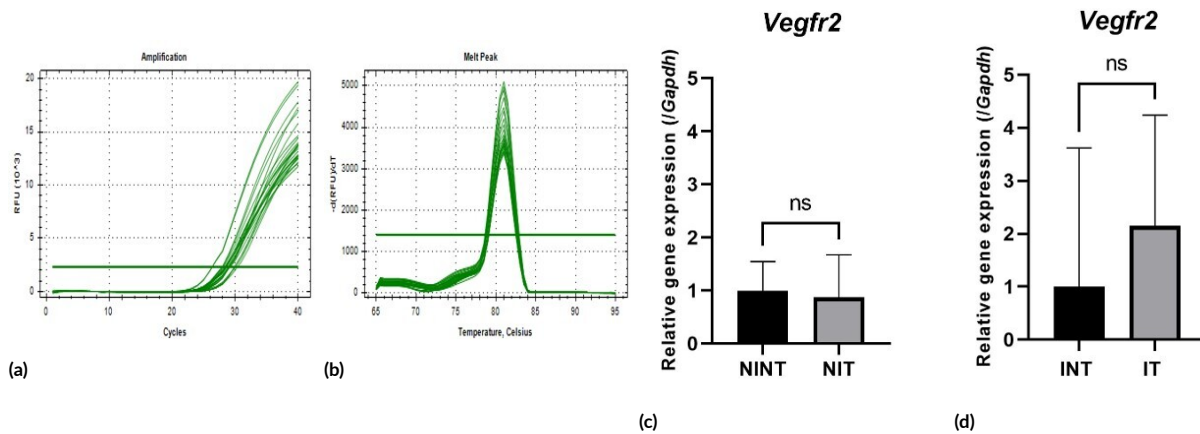
FIGURE 2 Relative gene expression of *Vegfr2* in normal breast and breast tumors after ECCT therapy. Amplification and melt peak chart of *Vegfr2* (2a and 2b). Relative gene expression of *Vegfr2* (2c and 2d). The internal control of relative gene expression is *Gapdh*. Independent t-test, ns = not significant ($p > 0.05$). NINT= non-DMBA-induced, non-ECCT-therapied rats; NIT= non-DMBA-induced, ECCT-therapied rats; INT= DMBA-induced, non-ECCT-therapied rats; IT= DMBA-induced and ECCT-therapied rats. The error bar indicates a standard deviation of three biological replications with two technical replications.
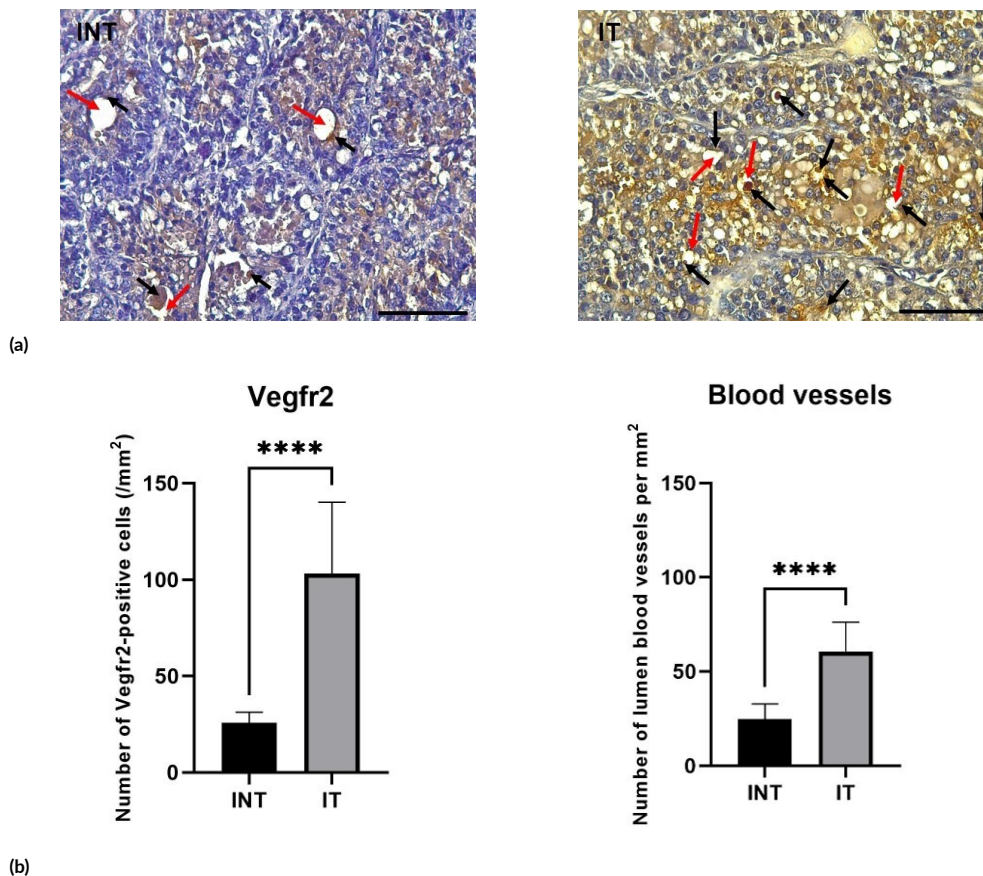
FIGURE 3 a. Immunostaining of Vegfr2 in breast tumor (INT) and after ECCT therapy (IT). b. Statistical results of Vegfr2-positive cells per mm^2 and the number of lumens per mm^2. The histological slide was observed using Leica CC50 E at 1 μm/pixel resolution at 400X magnification. Scale bar = 400 μm. Independent t-test; ****, $p < 0.0001$. Vegfr2-positive cell (black arrow), blood vessel (red arrow). INT= DMBA-induced, non-ECCT-therapied rats, IT= DMBA-induced and ECCT-therapied rats. The error bar indicates a standard deviation of 3 replications (30 field of view of each replication).

3.4. Discussion

Angiogenesis mechanism of the normal breast tissue and DMBA-induced rat breast tumor, with and without ECCT therapy, has been examined in this research. Our findings suggest ECCT is safe for normal breast tissue angiogenesis (Figure 1g, 1h, 1i, 2c). Angiogenesis is the mechanism that responds to tumor hypoxia (Zimna and Kurpisz 2015). Thus, the healthy breast tissue with normoxia will express

normal angiogenic genes with or without ECCT exposure. This result supports the previous study that ECCT of 150 kHz and 18 Vpp did not affect normal breast tissue morphology (Pratiwi et al. 2019), as well as ECCT of 100 kHz and 18 Vpp (Alamsyah et al. 2021).

During breast tumor angiogenesis, *Hif1α* plays an essential role as a transcription factor for VEGF expression (Zimna and Kurpisz 2015). *Hif1α* existence is regulated by *prolyl-4-hydroxylase* (PHD). This enzyme inhibition will block the binding between the *von Hippel-Lindau* protein and *Hif1α*. Thus, the *Hif1α* could not be degraded by the proteasome (Zimna and Kurpisz 2015). Then, this *Hif1α* will be translocated to the nucleus to carry out its role as a transcription factor for *Vegfa* expression (Zimna and Kurpisz 2015). With consequences, the increasing *Hif1α* will be followed by increasing *Vegfa* (Zimna and Kurpisz 2015), wich was in-line with result of both gene expressions in the INT group (Figure 1g and 1i). However, ECCT exposure on rat breast tumor gave rise to distinct impacts on both gene expression, since Vegfa has been downregulated significantly, while *Hif1α* was not.

In this study, Vegfa gene expression in the ECCT-treated breast tumors may be influenced by the ECCT effect. Previous studies showed that ECCT of 150 kHz and 18 Vpp had anti-mitotic and pro-apoptotic effects in breast tumors, and the cell death of the ECCT-exposed breast tumors was predominated by apoptosis via the Caspase-3 pathway (Pratiwi et al. 2019). This fact may contribute to the current result, since Vegfa is the primary growth factor (Claesson-Welsh 2016), produced by hypoxia-tumor cells (Zimna and Kurpisz 2015). Thus, cell death by ECCT exposure has reduced *Vegfa* gene expression. Another study has proved that Caspase-3 upregulation and downregulation of Vegfa in training-treated mice breast tumors may have an impact on reducing tumor size (Rafiei et al. 2021).

However, significant downregulation of *Vegfa* in the ECCT-treated breast tumor is inconsistent with *Hif1α* expression. *Hif1α* plays a role as a transcription factor to determine other target genes related to homeostasis (Corrado and Fontana 2020). Therefore, we argue that distinct cells may express this gene, besides tumor cells. In addition, *Hif1α* may have other roles in regulating tissue homeostasis, particularly in determining other angiogenic growth factors. The multifunction of Hif1α is also proven by its contribution to T-cell differentiation and function (Palazon et al. 2017).

The expression of *Sp1*, another transcription factor, was similar among the groups. In the *Hif1α-independent* pathway, *Sp1* is the transcription factor that regulate *Vegfa* expression (Karar and Maity 2011; Vellingiri et al. 2020). However, based on the result, this factor seems not to regulate *Vegfa* expression.

The most prominent result in this study is the correlation of *Vegfa* and *Vegfr2* expression. *Vegfa* subtype is the primary signal during tumor angiogenesis and *Vegfr2* is its specific receptor (Claesson-Welsh 2016). During angiogenesis, the *Vegfa/Vegfr2* signaling pathway is the signal transduction (Abhinand et al. 2016) to induce endothelial

cell proliferation, migration, permeability, and survival (Guo et al. 2010).

The conventional model of ligand-induced dimerization and activation is believed to play a role in angiogenesis. Thus, protein Vegfr2 is monomeric (Vegfr2 without ligand) and has no angiogenic capacity (Abhinand et al. 2016). Interestingly, this study showed that *Vegfa* expression was in contrast to its receptor expression in the ECCT-treated breast tumor. ECCT exposure induced blood vessel development in rat breast tumor, following upregulated Vegfr2 expression instead of following *Vegfa* as an angiogenic growth factor.

Eguchi et al. (2022) have reviewed the angiogenesis mechanism involving both *Vegfs/Vegfr2*-dependent and *Vegfs/Vegfr2*-independent pathways. The latter is possible without *Vegfa/Vegfr2* signaling. In this condition, Vegfa-independent angiogenic factors take over its role (Eguchi et al. 2022). A previous study has proven that ligand-independent dimerization regulated Vegfr2 dimerization and activation by Ig-like Domain 4 in HUVECs and breast cancer cells (Zhang et al. 2017). Therefore, the increasing blood vessels in the ECCT-treated breast tumor might be induced by Vegfr2 dimerization, regulated by the presence of Ig-like Domain 4 on the Vegfr2 extracellular domain. However, further research is necessary to prove electric field produced from ECCT could trigger Vegfr2 dimerization.

On the other hand, direct current (DC)-electric fields induced angiogenesis by increasing the *Vegf* of endothelial cells and its regulation involving *Vegfr2* (Chen et al. 2018). Our findings show *Vegf* downregulation and Vegfr2 upregulation, as well as elevating new blood vessels only in the ECCT-exposed rat breast tumors. Both electric field sources indicate the vital role of Vegfr2 during blood vessel development. Hence, Vegfr2-dependent angiogenesis may be the main pathway in ECCT-treated breast tumor angiogenesis.

A review stated that the activation of abnormal receptor tyrosine kinase (RTK) in cancer possibly occurred through one or more of these mechanisms, i.e. gain-of-function mutations, genomic amplification, chromosomal rearrangement, and/or autocrine activation (Du and Lovly 2018). Vegfr2 is one of the RTK members. Thus, overexpression of Vegfr2 in ECCT-treated breast tumors may be mediated by those mechanisms. However, no previous data reported the AC electric field effect on the receptor during tumor angiogenesis.

This study showed that ECCT induced rat breast tumor angiogenesis, and according to the hallmark of cancer, it is a characteristic of worse prognosis. Since new blood vessels may induce cancer progression and metastasis (Hanahan and Weinberg 2000). However, considering that cancer is characterized by multiple hallmarks, it should be studied comprehensively and deeply. Previous research has shown that ECCT 150 kHz promoted immune response in rat breast tumors, by inducing macrophage CD68 (Pratiwi et al. 2019) and CD8 lymphocyte (Nuriliani et al. 2024). ECCT 100 kHz also has upregulated lympho-

cyte CD8 (Alamsyah et al. 2021). Those data show that new blood vessels may facilitate immune cell migration to infiltrate the tumor, thus promoting the immune system against tumor. It was proven by Tumor Interstitial Fluid (TIF), which makes tumor morphology soft and fluid after ECCT exposure (Pratiwi et al. 2019), and TIF contains stromal and immune cells (Wagner and Wiig 2015).

Lastly, angiogenesis is a complex mechanism involving several pathways in normal physiology and pathology conditions. The obtained data in this study does not adequately understand the angiogenesis mechanism in ECCT-exposed breast tumors. Therefore, further research is essential to complete the angiogenesis mechanism puzzle. However, this pre-clinical result may become basic information for clinical research to support ECCT as a novel breast tumor therapy modality.

4. Conclusions

ECCT has no effects on normal breast tissue angiogenesis. ECCT upregulated *Vegfr2* expression and increased the number of blood vessels in breast tumors, but contrasting with the downregulated *Vegfa* expression. It suggests that ECCT may induce breast tumor angiogenesis by the Vegfr2-dependent angiogenesis pathway

Acknowledgments

Authors' contributions

ESP carried out the laboratory work, collected the data, performed the data analysis, and wrote the manuscript. BRA wrote the manuscript. PA wrote the manuscript. FA wrote the manuscript and provided resources (ECCT device). WPT provided resources (ECCT device). RP designed the study, performed the data analysis, and wrote the manuscript. All authors read and approved the final version of the manuscript.

Competing interests

We declare that there is no conflict of interest to disclose regarding this manuscript.

References

Abhinand CS, Raju R, Soumya SJ, Arya PS, Sudhakaran PR. 2016. VEGF-A/VEGFR2 signaling network in endothelial cells relevant to angiogenesis. J. Cell Commun. Signal. 10(4):347–354. doi:10.1007/s12079-016-0352-8.

Alamsyah F, Ajrina IN, Nur F, Dewi A, Iskandriati D, Prabandari SA, Taruno WP. 2015. Antiproliferative effect of electric fields on breast tumor cells *in vitro* and *in vivo*. Indones. J. Cancer Chemoprevention 6(3):71–77.

Alamsyah F, Fadhlurrahman A, Pello J, Firdausi N, Evi S, Karima F, Pratiwi R, Fitria L, Nurhidayat L, Taruno W. 2018. PO-111 Non-contact electric fields inhibit the growth of breast cancer cells in animal models and induce local immune reaction. ESMO Open 3:A269. doi:10.1136/esmoopen-2018-eacr25.636.

Alamsyah F, Pratiwi R, Firdausi N, Irene Mesak Pello J, Evi Dwi Nugraheni S, Ghitha Fadhlurrahman A, Nurhidayat L, Purwo Taruno W. 2021. Cytotoxic T cells response with decreased CD4/CD8 ratio during mammary tumors inhibition in rats induced by non-contact electric fields. F1000Research 10:35. doi:10.12688/f1000research.27952.1.

Chen Y, Ye L, Guan L, Fan P, Liu R, Liu H, Chen J, Zhu Y, Wei X, Liu Y, Bai H. 2018. Physiological electric field works via the VEGF receptor to stimulate neovessel formation of vascular endothelial cells in a 3D environment. Biol. Open 7(9):bio035204. doi:10.1242/bio.035204.

Claesson-Welsh L. 2016. VEGF receptor signal transduction – A brief update. Vascul. Pharmacol. 86::14–17. doi:10.1016/j.vph.2016.05.011.

Corrado C, Fontana S. 2020. Hypoxia and HIF signaling: One axis with divergent effects. Int. J. Mol. Sci. 21(16):1–17. doi:10.3390/ijms21165611.

Du Z, Lovly CM. 2018. Mechanisms of receptor tyrosine kinase activation in cancer. Mol. Cancer 17(1):1–13. doi:10.1186/s12943-018-0782-4.

Eguchi R, Kawabe JI, Wakabayashi I. 2022. VEGF-independent angiogenic factors: Beyond VEGF/VEGFR2 signaling. J. Vasc. Res. 59(2):78–89. doi:10.1159/000521584.

Guntarno NC, Rahaju AS, Kurniasari N. 2021. The role of MMP-9 and VEGF in the invasion state of bladder urothelial carcinoma. Indones. Biomed. J. 13(1):61–67. doi:10.18585/inabj.v13i1.1348.

Guo S, Colbert LS, Fuller M, Zhang Y, Gonzalez-Perez RR. 2010. Vascular endothelial growth factor receptor-2 in breast cancer. Biochim. Biophys. Acta - Rev. Cancer 1806(1). doi:10.1016/j.bbcan.2010.04.004.

Hanahan D. 2022. Hallmarks of cancer: New dimensions. Cancer Discov. 12(1):31–46. doi:10.1158/2159-8290.CD-21-1059.

Hanahan D, Weinberg RA. 2000. The hallmarks of cancer. Cell 100(1):57–70. doi:10.1016/S0092-8674(00)81683-9.

Karar J, Maity A. 2011. PI3K/AKT/mTOR pathway in angiogenesis. Front. Mol. Neurosci. 4:1–8. doi:10.3389/fnmol.2011.00051.

Kim EH, Song HS, Yoo SH, Yoon M. 2016. Tumor treating fields inhibit glioblastoma cell migration, invasion and angiogenesis. Oncotarget 7(40):65125. doi:10.18632/oncotarget.11372.

Kobori T, Hamasaki S, Kitaura A, Yamazaki Y, Nishinaka T, Niwa A, Nakao S, Wake H, Mori S, Yoshino T, Nishibori M, Takahashi H. 2018. Interleukin-18 amplifies macrophage polarization and morphological alteration, leading to excessive angiogenesis. Front. Immunol. 9(MAR):334. doi:10.3389/fimmu.2018.00334.

Livak KJ, Schmittgen TD. 2001. Analysis of relative gene expression data using real-time quantitative PCR and the 2-$\Delta\Delta$CT method. Methods 25(4):402–408. doi:10.1006/meth.2001.1262.

Nuriliani A, Nurhidayat L, Fatmasari H, Afina D, Alamsyah F, Taruno WP, Pratiwi R. 2024. Non-contact electric field may induced higher CD4, CD8, Caspase-8, and Caspase-9 protein expression in breast tumort tissue of rats (*Rattus norvegicus* Berkenhout, 1769). Malaysian J. Fundam. Appl. Sci. 20(1):74–88. doi:10.11113/mjfas.v20n1.3065.

Palazon A, Tyrakis PA, Macias D, Veliça P, Rundqvist H, Fitzpatrick S, Vojnovic N, Phan AT, Loman N, Hedenfalk I, Hatschek T, Lövrot J, Foukakis T, Goldrath AW, Bergh J, Johnson RS. 2017. An HIF-1α/VEGF-A axis in cytotoxic T cells regulates tumor progression. Cancer Cell 32(5):669–683.e5. doi:10.1016/j.ccell.2017.10.003.

Pratiwi R, Antara NY, Fadliansyah LG, Ardiansyah SA, Nurhidayat L, Sholikhah EN, Sunarti S, Widyarini S, Fadhlurrahman AG, Fatmasari H, Tunjung WAS, Haryana SM, Alamsyah F, Taruno WP. 2019. CCL2 and IL18 expressions may associate with the anti-proliferative effect of noncontact electro capacitive cancer therapy *in vivo*. F1000Research 8:1770. doi:10.12688/f1000research.20727.1.

Rafiei MM, Soltani R, Kordi MR, Nouri R, Gaeini AA. 2021. Gene expression of angiogenesis and apoptotic factors in female BALB/c mice with breast cancer after eight weeks of aerobic training. Iran. J. Basic Med. Sci. 24(9):1196–1202. doi:10.22038/ijbms.2021.55582.12427.

Sung H, Ferlay J, Siegel RL, Laversanne M, Soerjomataram I, Jemal A, Bray F. 2021. Global Cancer Statistics 2020: GLOBOCAN estimates of incidence and mortality worldwide for 36 cancers in 185 countries. CA. Cancer J. Clin. 71(3):209–249. doi:10.3322/caac.21660.

Suvarna SK, Layton C, Bancroft JD. 2012. Bancroft's theory and practice of histological techniques, seventh edition. Philadelphia: Churchill Livingstone of El Sevier.

Vellingiri B, Iyer M, Subramaniam MD, Jayaramayya K, Siama Z, Giridharan B, Narayanasamy A, Dayem AA, Cho SG. 2020. Understanding the role of the transcription factor Sp1 in ovarian cancer: From theory to practice. Int. J. Mol. Sci. 21(3):1153. doi:10.3390/ijms21031153.

Wagner M, Wiig H. 2015. Tumor interstitial fluid formation, characterization, and clinical implications. Front. Oncol. 5(MAY):1–12. doi:10.3389/fonc.2015.00115.

Zhang S, Gao X, Fu W, Li S, Yue L. 2017. Immunoglobulin-like domain 4-mediated ligand-independent dimerization triggers VEGFR-2 activation in HUVECs and VEGFR2-positive breast cancer cells. Breast Cancer Res. Treat. 163(3):423–434. doi:10.1007/s10549-017-4189-5.

Zimna A, Kurpisz M. 2015. Hypoxia-Inducible factor-1 in physiological and pathophysiological angiogenesis: Applications and therapies. Biomed Res. Int. 2015:549412. doi:10.1155/2015/549412.